AIAA 98-2277

NONAXISYMMETRIC DISTURBANCES IN A JET AND THEIR EFFECT ON STRUCTURAL LOADING

A. Bayliss
Northwestern University, Evanston, IL

L. Maestrello
NASA Langley Research Center, Hampton, VA

4th AIAA/CEAS Aeroacoustics Conference
June 2-4, 1998 / Toulouse, France

NONAXISYMMETRIC DISTURBANCES IN A JET AND THEIR EFFECT ON STRUCTURAL LOADING

A. Bayliss *
Northwestern University, Evanston, IL

L. Maestrello †
NASA Langley Research Center, Hampton, VA

Abstract

A model of sound generated in a high subsonic (Mach 0.9) circular jet is solved numerically in cylindrical coordinates for nonaxisymmetric disturbances. The jet is excited by transient mass injection by a finite duration pulse via a rotating ring source. The flow field, near field and far field pressure disturbances corresponding to these sources are described. In particular, the resulting pressure field, which would serve to excite nearby panels, is illustrated together with preliminary results on the excitation of thin slices of nearby panels.

We consider both the short time behavior of the jet and the long time behavior, after the initial excitation pulse has exited the computational domain. The long time behavior of the jet is dominated by vorticity and pressure disturbances generated at the nozzle lip and growing as they convect downstream in the jet. These disturbances generate sound as they propagate. We find that rotating nonaxisymmetric disturbances persist for long times. Furthermore, depending on location, both in phase and out of phase behavior can be found upon reflection across the jet axis.

1 Introduction

In this paper, the generation and propagation of sound in a high subsonic jet excited by nonaxisymmetric disturbances is simulated. We consider a circular jet exiting from a straight nozzle extending to infinity in the upstream direction. The jet is excited by a nonaxisymmetric transient source and both the short time and long time behavior of the disturbance pressure is considered. We solve the full nonlinear Euler equations in conservation form modified so that a spreading jet profile, obtained from experimental measurements, is a solution in the absence of any disturbances.

The primary objectives are (i) to characterize nonaxisymmetric aspects of the flow field and near field and (ii) to characterize nonaxisymmetric effects in the far field. The jet is initially excited by a spatially and temporally localized source of transient mass injection. We consider a rotating modulated ring source for the excitation, thus generating a rotating nonaxisymmetric disturbance which propagates along the jet in a helical fashion. This leads to an initial acoustic disturbance which propagates through the jet. As a result of the excitation, instability waves are generated in the jet. These waves grow and then decay as they convect downstream, generating sound in the process. This phenomenon occurs over time scales much longer than that of the excitation pulse. The emphasis in this paper is on both the short time and the long time response of the jet, i.e., after the wave due to the excitation pulse has exited the domain of interest. Thus, instability wave generated sound in the jet is simulated. The simulation does not directly account for sound generated by small scale turbulent sources in the jet.

In previous work we have considered jet acoustics for circular jets subject to both axisymmetric and nonaxisymmetric disturbances. In particular, both linear and nonlinear responses have been considered.[1, 2, 3, 4] In these references the jet is excited by a source of transient mass injection and the development of instabilities together with associated sound generation is computed. The results in these references demonstrate the properties of instability wave generated sound. A succession of disturbances is generated at the nozzle lip. These disturbances initially grow as they convect in the jet. As they grow they generate pressure disturbances

*Professor, Dept. of Eng. Sciences & Appl. Math.
†Senior Staff Scientist, Associate Fellow AIAA

which propagate into the far field as sound. The far field radiation peaks at about 30° from the jet axis in agreement with measurements and observations. Flapping modes, obtained from static modulated ring sources have also been computed. In these modes regions of large pressure alternate on different sides of the jet.[4]

We have also considered two dimensional Cartesian jets.[5, 6, 7, 8] In two dimensions we have computed both the sound generated from instability waves and the interaction of this sound with a nearby flexible structure. These computations spanned a range of jet velocities up to and including supersonic jets. The two dimensional results for high subsonic jets (the parameter range considered here) indicated that the long time behavior of the excited jet is dominated by a nearly periodic acoustic response at a particular fundamental frequency together with harmonics.[7] Peak radiation is beamed at approximately 30° from the jet axis. The unsteady flow field is dominated by disturbances generated at the nozzle lip and propagating along the jet. In contrast to the nearly periodic far field, the flow field exhibited an aperiodic, apparently chaotic behavior.

The exact sources of jet noise have been identified from the basic equations of fluid dynamics.[9, 10, 11, 12, 13] Computation of the exact sources would require solution of the Navier-Stokes equations in the jet accompanied by an appropriate turbulence model. Such computations are difficult to conduct, particularly in three dimensions. Both small scale and large scale disturbances in the jet can act as sources of sound. In this paper we consider only sound generated from large scale instability waves. These instability waves are generated within the transiently excited jet by the mechanism described above.

Instability waves or large scale structures which can act as sources of sound in a jet have been observed in experiments[1, 14, 15] and studied by analytical[16, 17, 18, 19, 20, 21, 22] and numerical[1, 1, 3, 23] methods. While there have been a limited number of three dimensional computations [24, 25], the cost of the 3D computations has to date precluded a detailed study of the role of nonaxisymmetric large scale structures as sources of jet noise and has generally forced restrictive assumptions such as linearity. On the other hand, many of the large scale structures observed in experiments are intrinsically nonaxisymmetric, e.g., helical and flapping modes, and thus a full understanding of jet acoustics requires an understanding of nonaxisymmetric modes in the jet and the resulting acoustic radiation. This is particularly true when the unsteady pressure in the jet serves to load nearby panels. In this case, the panel response can crucially depend on the nature of the nonaxisymmetric disturbances.

In our model we solve a modified version of the full nonlinear Euler equations in cylindrical geometry. The equations are modified to account for a spreading jet as described below. As a result, the inviscid, instability wave sources of sound are computed directly together with the resulting sound generation. We specifically include a straight nozzle from which the jet exits. The flow field and near field disturbances are computed together with the far field sound radiation.

2 Model and Numerical Method

The computational domain is shown in Figures 1a. We consider a jet exiting from a straight, circular pipe of diameter D, where $D = 4$ inches. All boundaries are artificial boundaries at which radiation boundary conditions are employed.[1, 28] In these computations we employ an adaptive radiation boundary condition in that the assumed origin of coordinates is adaptively chosen so as to minimize a measure of the error of the boundary condition. The jet is excited by a transient source of mass injection located approximately $1D$ downstream from the nozzle exit. This source is both spatially and temporally localized, leading to a broad band excitation. Unsteady pressure, density and velocity are computed both interior and exterior to the pipe. This leads to the generation of a train of instability waves which propagate along the jet, decaying beyond the potential core of the jet and generating sound.

The primary objective is to consider the loading on nearby panels due to the jet pressure. Some limited results along this line are presented below. In Figure 1b we sketch the desired configuration.

The Euler computations employ a (2-4) version of the MacCormack scheme.[26] Further details on the numerical scheme are given in the references.[5, 6, 7] The spatial fourth order accuracy is necessary in order to follow the acoustic waves over large distances without undue numerical dispersion. This is particularly important given the coarse grids necessitated by nonaxisymmetric computations.

The Euler equations are solved in conservation form in cylindrical coordinates z, r, ψ, where z denotes the axial distance, r the radial distance and ψ is the azimuthal angle. The dependent variable is the vector

$$\hat{\mathbf{q}} = (\rho, \rho u, \rho v, \rho w, E)^T,$$

where ρ is the density, u, v and w are the axial, radial and azimuthal velocity components respectively, and E is the total energy per unit volume. The pressure, p, is obtained from the equation of state.

The Euler equations are modified in the jet domain to account for the jet flow. The jet exits from a nozzle of diameter D located at $z = 0$ and the solution is computed both within and exterior to the nozzle. The Euler equations are modified to account for two different non-homogeneous forcing terms.[7] One term serves as an excitation pulse to excite the jet. It corresponds to a localized source of mass injection. In axisymmetric computations we take a point source centered on the axis at z_s. In the non-axisymmetric computations we consider a rotating ring source of radius r_s, where $r_s \simeq .3D$. For each ψ the source is a peaked Gaussian centered at r_s, z_s. The amplitude of the source is modulated The temporal dependence of the source is described in the references, e.g., [5]. The amplitude of the source is modulated by the function $1 + \epsilon_1 \cos(\psi + \omega t)$ where $\epsilon_1 = 0.125$. Thus, the modulation represents a spinning excitation and serves to excite a spinning mode in the jet. The source is localized in time, thus leading to broad band excitation.

The second forcing term is designed so that in the absence of the excitation pulse the solution to the Euler equations would be a stationary profile corresponding to a spreading jet. In the present computation, mean density and pressure are assumed constant, as are the mean radial and azimuthal velocities. The mean axial velocity U is a taken from experimental measurements and models an isothermal jet with exit Mach number 0.9. [27]

The inclusion of this term separates the computation of the disturbance, in particular the resulting instability waves, from the computation of the mean flow (i.e. the spreading jet). Thus, the resulting system of equations allows for the simulation of instability waves and the resulting sound generation, together with the propagation of acoustic waves in the jet flow field, without requiring the computation of the spreading jet itself. Although this is a simplified model, it captures many of the observed features of instability wave generated jet sound and permits high resolution computation of the coupling of jet noise with the flexible panels and the resulting radiation from the panels. In particular, the model allows for computation of many of the natural sources of jet noise (the instability waves) together with the sound radiated by these sources.

3 Numerical Results

We first consider the nature of the unsteady pressure in the excited jet. We describe the far field, near field and flow field disturbance pressure $p = p(t, r, z, \psi) - p_\infty$ where p_∞ is the ambient pressure. We do not consider a fully coupled response of the structure, so the unsteady pressure field, computed without the structure, will serve as the excitation pressure for the nearby panel.

In response to the excitation source an initial acoustic wave emanates from the source location through the jet. Over short times this wave is the predominant feature in the unsteady flow field. However, this disturbance propagates essentially at the speed of sound and rapidly propagates out of the computational domain. A large slowly moving structure, an instability wave, is generated by the excitation pulse and propagates downstream along the jet axis. The long time behavior of the jet is dominated by a shedding of disturbances from the nozzle lip, the propagation of these disturbances downstream and the generation of sound from these disturbances as they grow and decay along the jet. We note that there are also disturbances that propagate upstream inside the pipe.

We first illustrate the structure of the fluctuating pressure field. Figures 2 and 3 are color contour plots for p in the $r - z$ plane $\sin(\psi) = 0$, i.e., the pressure field for the angles $\psi = 0$ and $\psi = \pi$. The coloring is according to the spectrum with red indicating large positive values of p and violet indicating large negative values of p. Note that colors are assigned based on a logarithmic scale. These contours are shown in Figures 2 and 3 at times $t_1 = 14.8$ and $t_2 = 16.6$ respectively, where the nondimensional time t is defined by $t = \tilde{t}c_\infty/L$, where $\tilde{t}$ is dimensional time, c_∞ is the ambient sound speed and the reference length L is 1 foot ($3D$).

In interpreting these figures, we recall that the nozzle exit is at $z = 0$ and the initial source was a ring source centered approximately $1D$ downstream of the nozzle exit and of approximately $0.5D$ in radius.

The initial acoustic disturbance due to the excitation pulse is still present in Figure 2. In addition, there is an array of acoustic disturbances propagating upstream both above and below the jet. Acoustic disturbances propagating up the nozzle can also be seen. These disturbances travel slowly, due to the nearly sonic velocity (Mach number 0.9) within the pipe. There is an array of large scale structures propagating along the jet axis with acoustic disturbances emanating from them. These disturbances

grow and then decay as they propagate along the jet.

At time t_2, corresponding to Figure 3, the initial acoustic wave has exited the computational domain. Additional large scale structures propagating along the jet axis have been generated, while those structures in Figure 2 have propagated further downstream, exhibiting a pronounced decay. In addition, there is a pronounced beaming of acoustic radiation at approximately 30° from the jet axis below the jet (i.e., in the half plane $\psi = \pi$).

We next illustrate different aspects of the unsteady pressure field. We first consider the far field pressure. In Figure 4 we plot p as a function of t for two different far field points. Both points are taken at 30° from the jet axis, however they are at opposite sides of the jet. Figure 5 is similar except that we consider points at 90° from the jet axis. Both figures are of the full time trace, including both the early and late time pressure. However, the predominant feature in the figures is the early time pressure corresponding to the excitation source. The pressure is greater below the jet, i.e., at $\psi = \pi$. This indicates that the predominant radiation from the excitation pulse occurs when the ring source has rotated so that maximum radiation occurs in the $\psi = \pi$ half plane.

We next focus on the late time behavior of the jet by considering the time interval $12 \leq t \leq 20$ after the initial pulse has exited the computational domain. We plot in Figure 6 the time history over this interval. There is an irregular oscillation in the pressure. We note that this oscillation is out of phase between $\psi = 0$ and $\psi = \pi$. Furthermore, the difference in level between $\psi = 0$ and $\psi = \pi$ is no longer the same as for the initial pulse. Indeed, the overall sound pressure level, obtained from integrating p^2 in time is higher at $\psi = 0$ than for $\psi = \pi$. This is shown in Figure 7 where the overall sound pressure level over this time interval is plotted against the far field angle for the half planes $\psi = 0$ and $\psi = \pi$. The data in the figure is normalized to 0 db for 90° for $\psi = 0$.

Thus the effect of the rotating source is to significantly enhance the differences in the initial pulse, depending on what plane has a maximal source at the time of maximal radiation. However, nonaxisymmetric behavior in both amplitude and phase persists to late times after the excitation pulse has exited the computational domain.

We next consider the near field pressure. In Figure 8 we plot the late time pressure at approximately $3D$ downstream and approximately $5D$ from the jet axis. In contrast to the far field pressure, the pressure oscillations are now *in phase* for the half planes $\psi = 0$ and $\psi = \pi$. There is also a long wavelength modulation in the relationship between the amplitude of p between the two half planes so that initially p in the half plane $\psi = \pi$ is greater than at the corresponding point in the half plane $\psi = 0$. The relative amplitudes then switch so that the pressure in the half plane $\psi = 0$ is greater and then they switch back again. We believe that this is a residual effect of the rotation of the excitation source.

We next consider the flow field pressure. In Figure 9 we plot p at approximately six diameters downstream and one diameter from the jet axis. There is a nearly sinusoidal oscillation which is again *in phase* for the two half planes. There is again a long time scale modulation for the relative amplitudes of the pressure between the 2 half planes.

We next illustrate the persistence of the rotating nature of the disturbance in Figure 10 where we plot the axial velocity w as a function of the cylindrical angle ψ for a range of values of t ($12 \leq t \leq 14.5$). The data is taken at approximately 1.5D downstream at a distance of $.5D$ from the jet axis. For these times the excitation pulse has long since decayed to zero. The figure shows an axial structure for w, which has completed approximately one full rotation within the time interval considered, thus illustrating the rotating nature of the long time solution.

We next consider the effect of the unsteady pressure on nearby flexible panels. In previous two dimensional computations we have considered a fully coupled model where both the panel response and radiation are computed simultaneously with the evolution of the unsteady pressure in the jet and are coupled to the computation of the pressure field in the jet. In view of the computational expense of the full three dimensional computations presented here, we consider a less complete model in which the pressure in the jet is first computed without the presence of the panel and is then used as a loading for a computation of panel response and radiation. Thus, the coupling between the panel radiation and the jet is neglected.

The loading pressure is computed as part of the jet computation described above. At present, we have only considered slices of 8 inch panels located along the axis of the jet at a height of $3D$ from the jet axis. We have computed the panel response to loading from the jet, employing parameters typical of aluminum. We illustrate this in Figure 11 where we plot the panel velocity vp as a function of t for two panels centered at $z = 0D$ and $Z = 6D$, respectively. There is a delayed response for the more downstream panel since it is at a great distance from

the jet source region. Furthermore, there is an increased emphasis of lower frequencies as the panel location shifts downstream.

Finally, we illustrate in Figure 12 the rotation of pressure disturbances in the jet where we show cross sections of the unsteady pressure as a function of r and ψ at a fixed z location (approximately $2D$ downstream from the nozzle). The diameter of the circular cross sections is approximately $1D$. The cross sections are shown for four different times, $t_a = 7.5$, $t_b = 9.3$, $t_c = 11.2$, $t_d = 13.0$, all of which are long after the excitation pulse has decayed to zero. The rotation of the pressure disturbance near the center of the jet can be clearly seen. We note that the rotation presented here is a different mode from the flapping modes described previously, where the nonaxisymmetry in the excitation source was stationary.[4]

4 Conclusion

We have developed a code to solve the nonlinear Euler equations for nonaxisymmetric disturbances in an axisymmetric jet. The code is second order in time and fourth order in space and is written in cylindrical coordinates with the cylindrical axis the axis of the jet. The simulation includes both the near and far field of the jet as well as the upstream region including a straight pipe from which the jet exits. The jet is excited by a transient ring source located near the nozzle exit with a rotating, nonaxisymmetric modulation. The long time behavior of the jet is dominated by a train of disturbances generated at the nozzle lip and propagating downstream along the jet. These disturbances in turn generate sound as they grow and decay in the jet shear layer.

The rotating nature of the unsteady flow field persists to late times, after the initial excitation pulse has decayed to zero. We have compared the disturbance pressure at different location in the computational domain, focusing on differences between the half planes $\psi = 0$ and $\psi = \pi$ where ψ is the cylindrical angle. The differences between these two half planes for the long time pressure depends on location. In the far field there is almost a 180° phase difference for the long time pressure oscillations between the two half planes. For near field locations, the pressure oscillations are in phase. For all points examined, there is a long time scale modulation in which the maximum pressure switches from one half plane to the other.

Preliminary investigations of the use of the computed jet pressure as loading for an array of flexible panels are presented. These results demonstrate the increased low frequency response as the downstream location of the panels increases.

Finally, examination of cross sections transverse to the jet axis indicates rotating pressure disturbances. These rotating disturbances are different from the flapping disturbances we have previously computed using excitation sources where the nonaxisymmetry was stationary.

Acknowledgments

AB was partially supported by NASA Langley Research Center under contract NAS1-19480 while in residence at ICASE. Additional support was provided by NSF grants DMS 93-01635 and DMS 95-30937.

References

[1] Maestrello, L., Bayliss, A. and Turkel, E., "On the Interaction of a Sound Pulse with the Shear Layer of an Axisymmetric Jet," *Journal of Sound and Vibration*, Vol. 74, 1981, pp. 281-301.

[2] Maestrello, L. and Bayliss, A., "Flowfield and Far Field Acoustic Amplification Properties of Heated and Unheated Jets," *AIAA Journal*, Vol. 20, 1982, pp. 1539-1546.

[3] Bayliss, A., Maestrello, L. and Turkel, E., "On the Interaction of a Sound Pulse With the Shear Layer of an Axisymmetric Jet, III: Non-Linear Effects," *Journal of Sound and Vibration*, Vol. 107, 1986, pp. 167-175.

[4] Bayliss, A. and Maestrello, L., "Response of High Subsonic Jet to Nonaxisymmetric Disturbances," AIAA paper 97-1580, 3rd AIAA/CEAS Aeroacoustics Conference, Atlanta, GA, May, 1997.

[5] McGreevy, J.L., Bayliss, A. and Maestrello, L., "Interaction of Jet Noise with a Nearby Panel Assembly," *AIAA Journal*, Vol. 33, 1995, pp. 577-585.

[6] Bayliss, A., Maestrello, L., McGreevy, J.L. and Fenno, C.C., "Forward Motion Effects on Jet Noise, Panel Vibration, and Radiation," *AIAA Journal*, Vol. 34, 1996, pp. 1103-1110.

[7] Fenno, C.C., Bayliss, A. and Maestrello, L., "Panel-Structure Response to Acoustic Forcing by a Nearly Sonic Jet," *AIAA Journal*, Vol. 35, 1997, pp. 219-227.

[8] Fenno, C.C., Bayliss, A. and Maestrello, L., "Interaction of Sound From Supersonic Jets With Nearby Structures," AIAA paper 97-0283, 35th Aerospace Sciences Meeting, Reno, NV, January, 1997.

[9] Lighthill, M.J., "On Sound Generated Aerodynamically-I, General Theory," *Proceedings of the Royal Society*, Vol. A222, 1954, pp. 1-32.

[10] Lilley, G.M., "Theory of Turbulence Generated Jet Noise: Generation of Sound in a Mixing Region," *U.S. Air Force Technical Report AFAPL-TR-72-53, IV*, Wright Patterson AFB, 1972.

[11] Ribner, H.S., "Dryden Lecture, Perspectives on Jet Noise," *AIAA Journal*, Vol. 19, 1981, pp. 1513-1526.

[12] Ribner, H.S., "Effects of Jet Flow on Jet Noise Via an Extension to the Lighthill Model," J. Fluid Mech., Vol. 321, 1996, pp. 1-24.

NASA Technical Memorandum 110163, 1995.

[13] Ffowcs Williams, J.E. and Kempton, A. J., "The Noise from the Large-Scale Structure of a Jet," *J. Fluid Mech.*, Vol. 84, 1975, pp. 673-694.

[14] Crow, S. and Champagne, F., "Orderly Structure in Jet Turbulence," *Journal of Fluid Mechanics*, Vol. 48, 1971, pp. 457-591.

[15] McLaughlin, D. K., Morrison, G.L. and Trout, T.R.,"Reynolds Number Dependence in Supersonic Jet Noise," *AIAA Journal*, Vol. 15, 1977, pp. 526-532.

[16] Bechert, D.W. and Pfizenmaier, E., "On the Amplification of Broadband Jet Noise by Pure Tone Excitation," *Journal of Sound and Vibration*, Vol. 43, 1975, pp. 581-587.

[17] Huerre, P. and Monkewitz, P. A., "Local and Global Instabilities in Spatially-Developing Flows," *Annual Review of Fluid Mechanics*, Vol. 22, 1990, pp. 473-537.

[18] Monkewitz, P. A., Berger, E. and Schumm, M., "The Nonlinear Stability of Spatially Inhomogeneous Shear Flows, Including the Effect of Feedback, " Eur. J. Mech. B/Fluids, Vol. 10, No. 2, 1991, pp. 295-300.

[19] Plaschko, P. "Helical Instabilities of Slowly Divergent Jets," J. Fluid Mech. B/Fluids, Vol. 92, 1979, pp. 209-215.

[20] Strange, P., J. R, and Crighton, D. G., "Spinning Modes On Axisymmetric Jets. Part I," J. Fluid Mech. B/Fluids, Vol. 134, 1983, pp. 231-245.

[21] Michalke, A. and Hermann, G., "On the Inviscid Instability of a Circular Jet With External Flow," *Journal of Fluid Mechanics*, Vol. 114, 1982, pp. 343-359.

[22] Michalke, A., "Survey on Jet Instability Theory," *Progress in Aerospace Science*, Vol. 21, 1984, pp. 159-199.

[23] Mankbadi, R., Hayder, M. and Povinelli, L., "The Structure of Supersonic Jet Flow and Its Radiated Sound," *AIAA Journal*, Vol. 32, 1994, pp. 897-906.

[24] Hixon, R, Shih, S. H. and Makbadi, R. R., "Direct Prediction of the Three Dimensional Acoustic Field of a Supersonic Jet Using Linearized Euler Equations, " AIAA paper 95-116, June, 1995.

[25] Bangalore, A., Morris, P. J. and Long, L.,N., "A Parallel Three Dimensional Computational Aeroacoustics Method Using a Nonlinear Disturbance Equation", AIAA Paper 96-1728, May, 1996.

[26] Gottlieb, D. and Turkel, E., "Dissipative Two-Four Methods For Time-Dependent Problems," *Mathematics of Computation*, Vol. 30, 1976, pp. 703-723.

[27] Maestrello, L., "Acoustic Energy Flow From Subsonic Jets and Their Mean and Turbulent Flow Structure," Ph.D. Thesis, University of Southampton, England, UK, 1975.

[28] Bayliss, A. and Turkel, E., "Radiation Boundary Conditions for Wave-Like Equations," *Communications on Pure and Applied Mathematics*, Vol. 33, 1980, pp. 707-725.

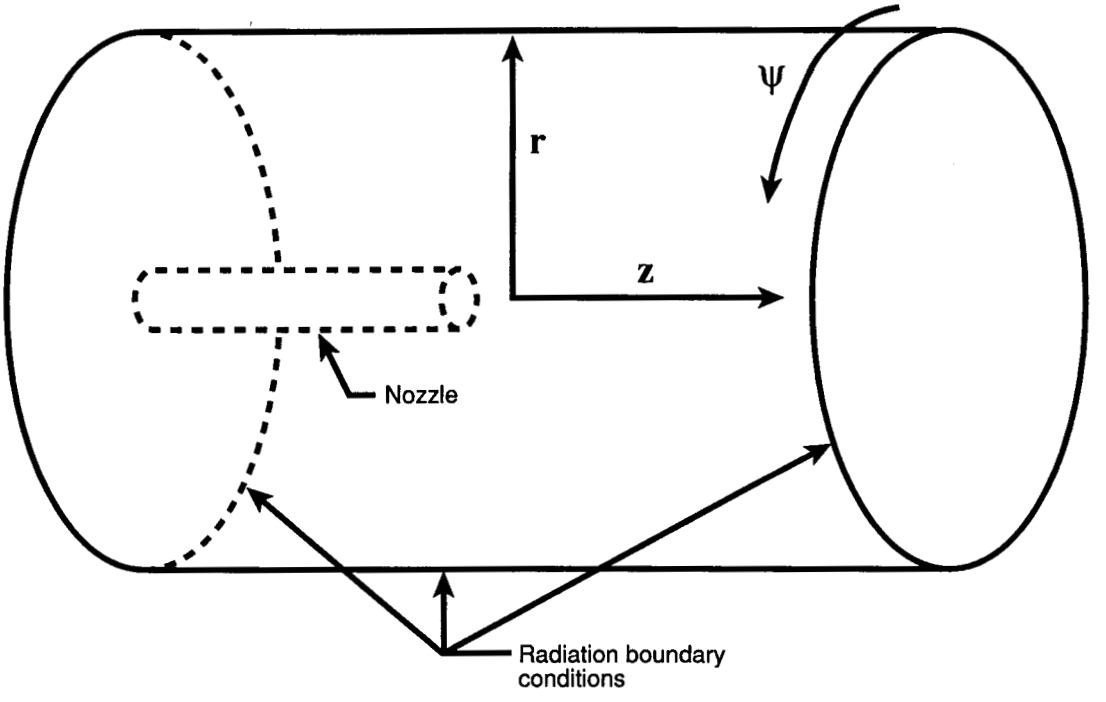

Figure 1a. Computational domain for cylindrical jet.

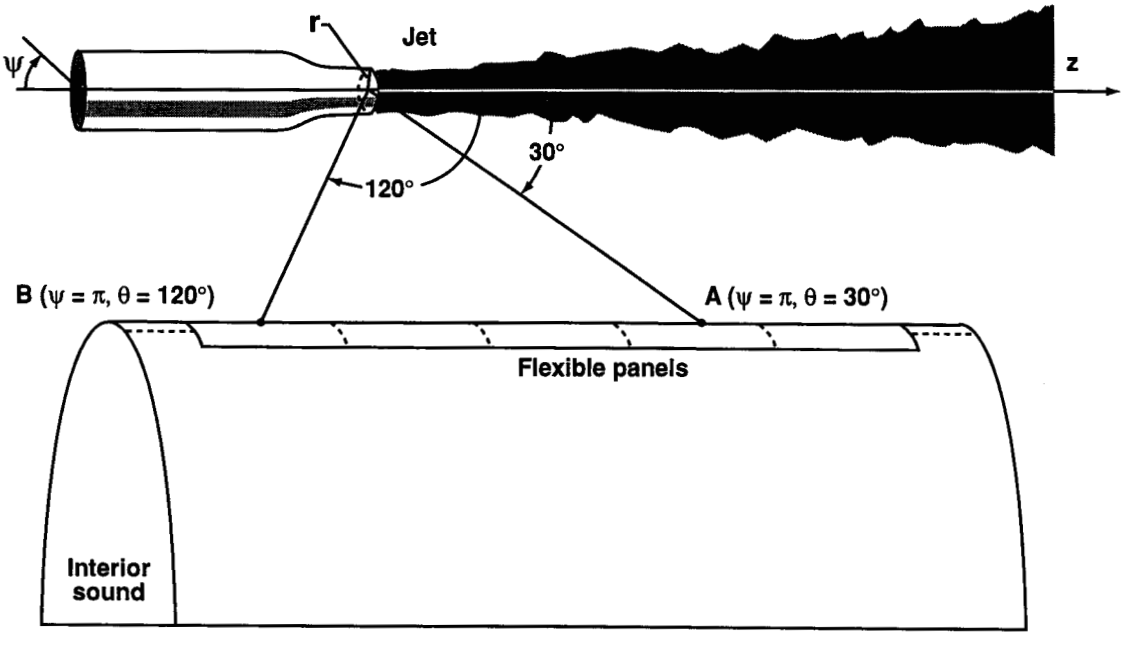

Figure 1b. Cylindrical jet with nearby structure.

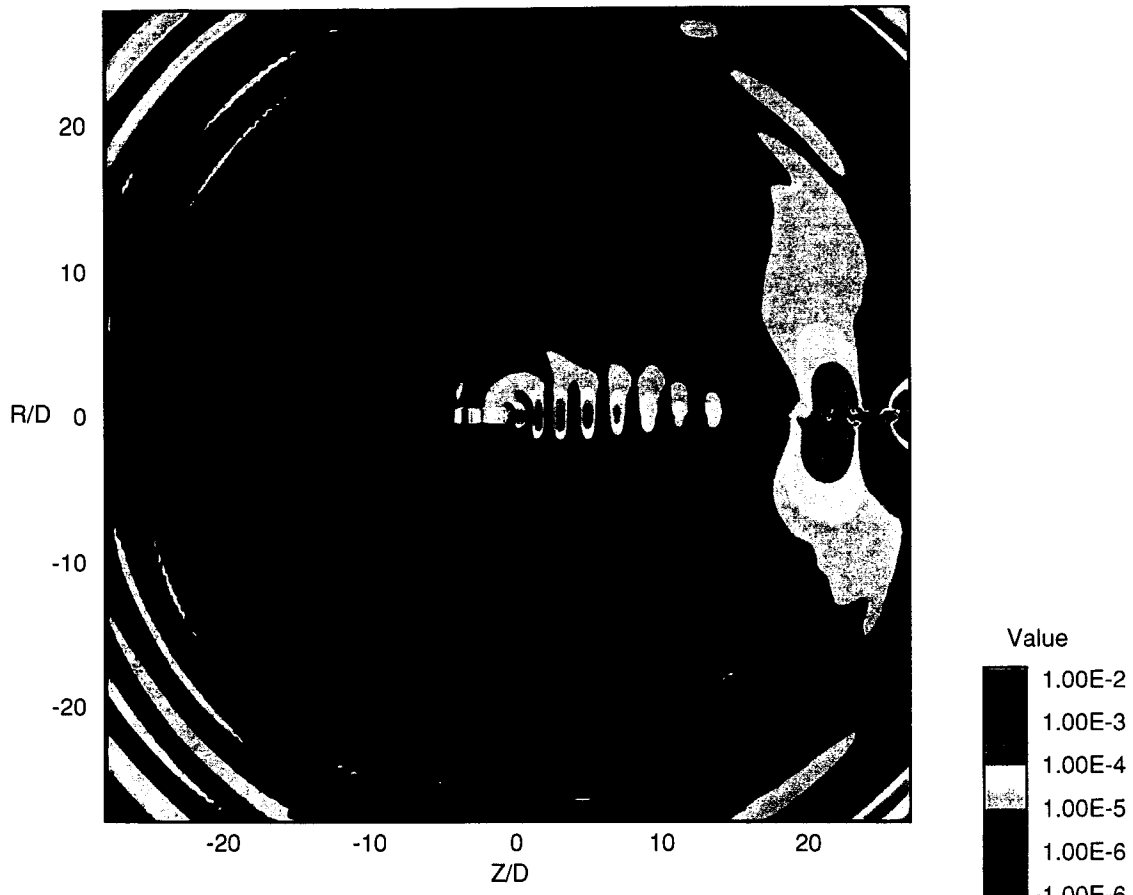

Figure 2. Color contour plot for p, t = 14.8

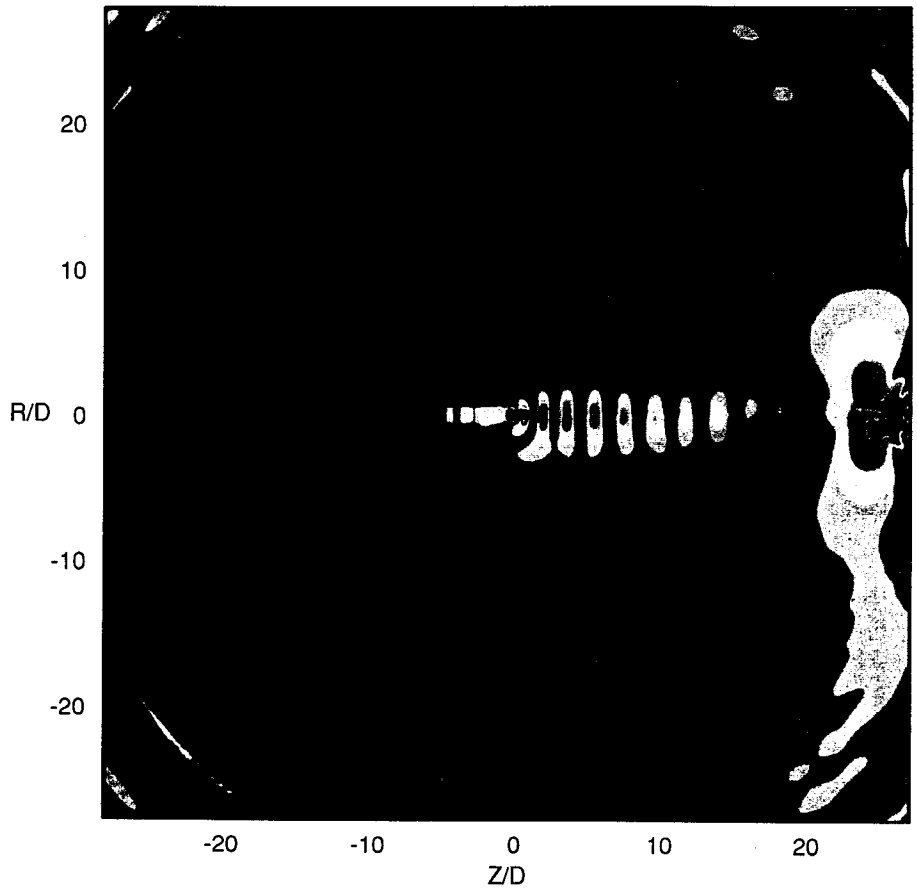

Figure 3. Color contour plot for p, t = 16.6

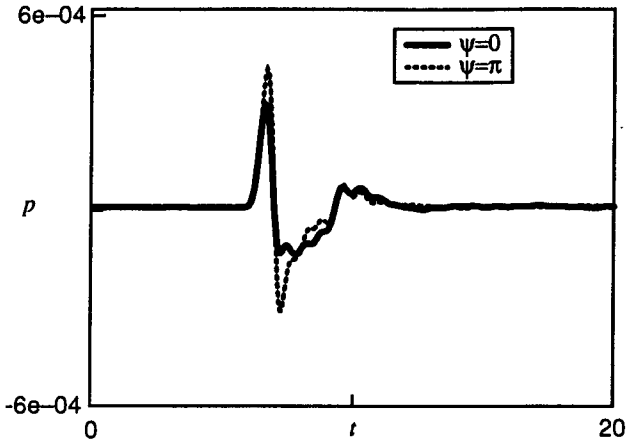

Figure 4. Far field pressure at 30°.

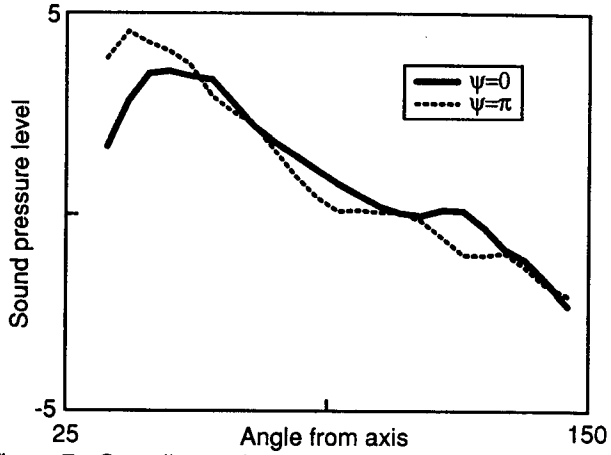

Figure 7. Overall sound pressure level over the time interval $12 \leq t \leq 20$ for the far field.

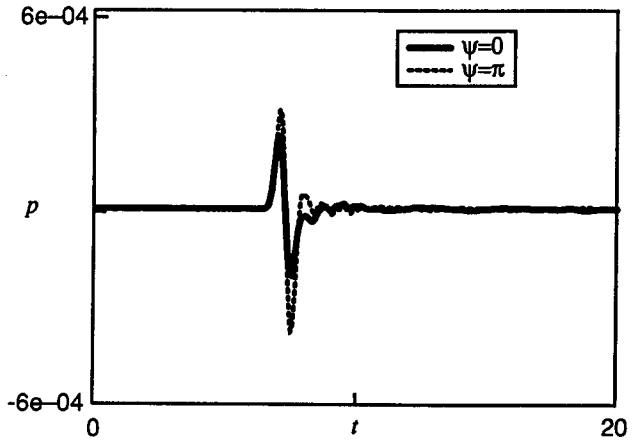

Figure 5. Far field pressure at 90°.

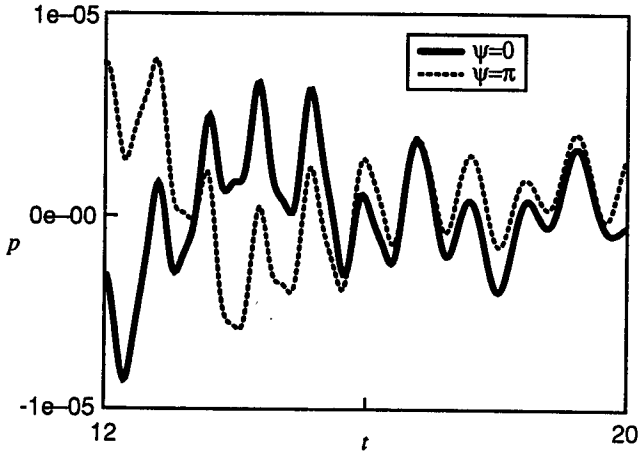

Figure 8. Near field pressure for $r \simeq 5D$ and $z \simeq 3D$, showing late time behavior.

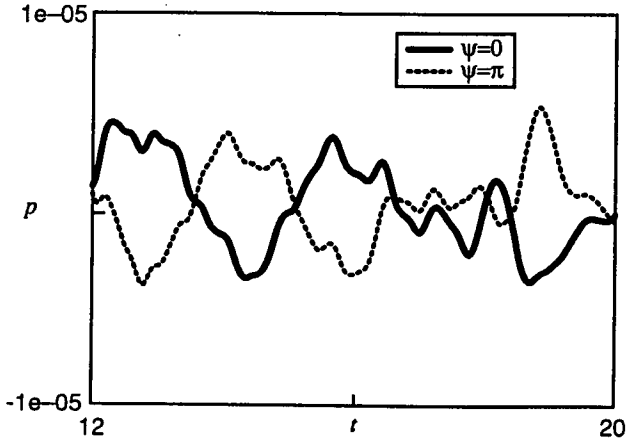

Figure 6. Far field pressure at 90° showing late time behavior.

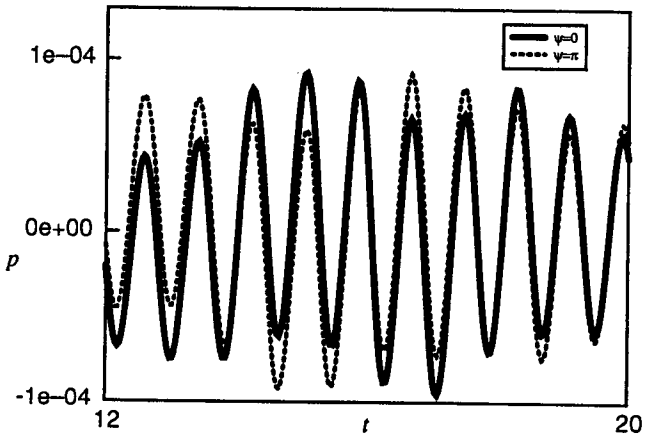

Figure 9. Flow field pressure for $r \sim D$ and $z \simeq 6D$, showing late time behavior.

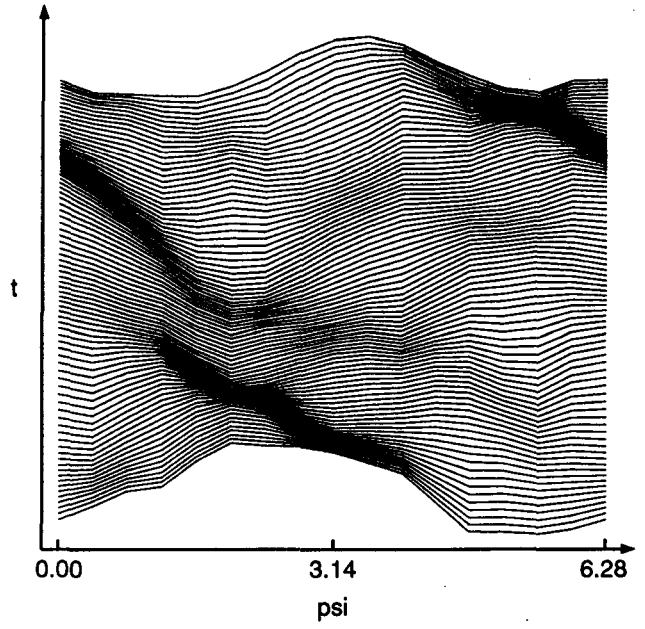

Figure 10. Azimuthal velocity $\tilde{w}$ plotted against ψ and t for $12 \leq t \leq 14.5$.

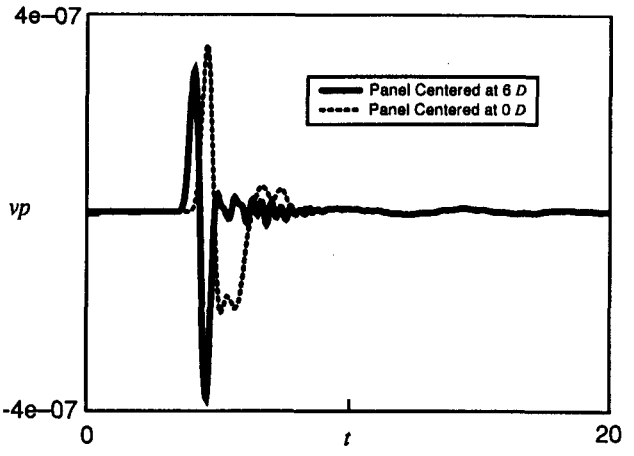

Figure 11. Panel normal velocity vp plotted against t for slices of two 8-inch panels located along the axis.

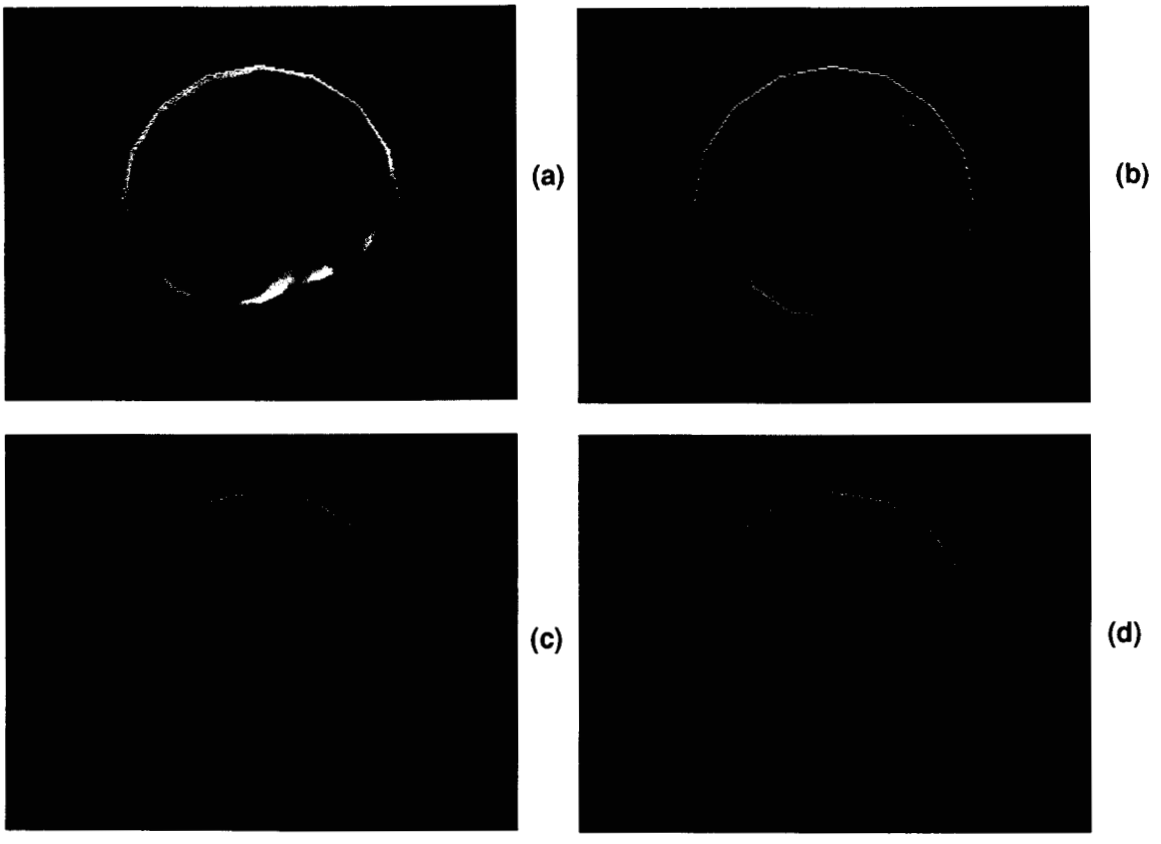

Figure 12. Axial cross sections of $\tilde{p}$ at four successive times (times indicated in text.)